Received: 30 January 2021 | Revised: 11 March 2022 | Accepted: 19 March 2022
DOI: 10.1111/vsu.13814

ORIGINAL ARTICLE - RESEARCH

WILEY

Compression generated by cortical screws in an artificial bone model of an equine medial femoral condylar cyst

Caitlin R. Moreno DVM[1] | **Elizabeth M. Santschi DVM, DACVS[1]** | **Jennifer Janes DVM, PhD, DACVP[2]** | **Jie Liu DDS, MS, PhD[3]** | **Do-Gyoon Kim PhD[3]** | **Alan S. Litsky MD, ScD[4,5]**

[1]Department of Clinical Sciences, Kansas State University, Manhattan, Kansas, USA
[2]Equine Programs, University of Kentucky, Lexington, Kentucky, USA
[3]Division of Orthodontics, The Ohio State University, Columbus, Ohio, USA
[4]Departments of Orthopaedics and Biomedical Engineering, The Ohio State University, Columbus, Ohio, USA
[5]Orthopaedic BioMaterials Laboratory, The Ohio State University, Columbus, Ohio, USA

Correspondence
Caitlin R. Moreno, Ohio State University Veterinary Medical Center, 601 Vernon L. Tharp Street, Columbus, OH 43210, USA.
Email: moreno.209@osu.edu

Funding information
Kansas State University

Abstract

Objective: Determine compression generated by lag and neutral screws over 12 h using two bone analogs.

Study design: Experimental study.

Sample population: Bone analogs were made of composite synthetic bone (CSB) or three-dimensional printed polylactic acid (PLA). Analogs had a 2 mm exterior shell with a 10 mm thick internal layer of open-cell material.

Methods: Bone analogs were opposed, making a 4-sided box with open ends. A central channel contained the sensor and the screws passed through it to engage both paired analogs. Four screw/analog conditions were tested: neutral and lag screw with bicortical engagement, neutral and lag screw with unicortical engagement. All screws were tightened to 2 Nm torque and compression values recorded at 0, 0.5, 1, 2, 6, and 12 h (six trials per condition). Medians were compared across groups for statistical significance.

Results: There was no difference in median compression between lag and neutral bicortical screws. For PLA, greater median compression was generated by neutral (median 437 N) and lag (median 379 N) bicortical screws compared to neutral unicortical screws (median 208 N, $p < .001$); lag bicortical screws generated greater median compression than lag unicortical screws (median 265 N, $p = .012$). For CSB, lag bicortical screws (median 293 N) generated greater median compression than neutral unicortical screws (median 228 N, $p = .008$).

Conclusion: Lag and neutral screws generated similar compression. Bicortical screws had higher median compression than unicortical screws in bone analogs.

Clinical significance: Neutral screws generate compression in cancellous bone analogs that can be increased with bicortical bone engagement.

1 | INTRODUCTION

Subchondral lucencies (SCL) are focal areas of cancellous and subchondral bone damage and loss, occurring most commonly in growing horses.[1] SCL can cause lameness and performance limitations. Traditional treatments of rest, anti-inflammatory therapies and surgical debridement can reduce lameness, but radiographic bone healing is infrequent.[2] A study in 2015 reported that placement of a transcondylar lag screw as a treatment for equine medial femoral condyle (MFC) SCL resulted in similar or superior rates of lameness resolution and bone healing,[3] and other studies reported similar results in other locations.[4,5] The proposed mechanism is that the SCL directs strain around the void and screws create a compressive force across the SCL, redirecting strain and resulting in bone formation stimulus.[6] The technique was developed empirically, as direct measurement of bone strain in the MFC is impossible. Subsequently, finite element analysis estimated bone strain around an MFC SCL[6] and the bone formation stimulus after screw placement and indicated that local bone mechanics play a role in the persistence and healing of SCL.[7] The use of a lag screw to provide compression across an SCL and redirect bone strain to stimulate bone formation on the inner surface is the proposed mechanism for bone healing.[7]

Lag screws are used in fracture repair to compress bone fragments,[8,9] but their use across an SCL has only been recently descibed.[3] Fully threaded screws used in lag fashion create compression when the tip end of the screw gains purchase in the far bone material and the screw head acts as a buttress.[8,9] The positive clinical results obtained after lag screw insertion in an MFC SCL[5] supports the clinical use of a lag screw to generate compressive force, but quantitative assessment of lag screw placement is surprisingly sparse in the literature.[10] For lag screws across MFC SCL, adequate MFC axial bone is necessary to achieve purchase of tip threads. One way to add more engaged bone is to place the screw in neutral fashion engaging bone on both sides of the void, but neutral screws are considered positional and do not provide compression.[9,11] Our clinical impression is neutral screws can generate compression in cancellous bone, for which there is experimental support.[12]

The objective of this study was to measure compression generated by 4.5 mm fully threaded cortical bone screws placed in neutral or lag fashion across an MFC SCL analog over 12 h. We hypothesized that both neutral and lag screws would generate compression which would be increased by engaging cortical bone analog on both sides of the void and that compression would decrease over time.

2 | MATERIALS AND METHODS

2.1 | Bone analogs

Artificial bone analogs were used to reduce the variability in bone density associated with cadaver bone and to allow a shape that accommodated the compression sensor. Two materials were used for the models, composite synthetic bone (CSB) and 3D, three-dimensional (3D) printed polylactic acid (PLA). Analogs had three sides: the largest was 80 × 63 mm and had two 6 × 80 mm walls on the long axis margins (Figure 1). The walls had an inner 10 mm of cancellous bone mimic and a 2 mm outer cortical bone mimic (Figure 1). The analogs were made with three sides to provide feedback resistance when compressed. One analog was inverted over a second and aligned in a bracket to form a 4-sided box with open ends (Figure 2) to allow the exit of a wire from the compression sensor to the digital gauge. The central void was 12 mm high, 40 mm wide, and 80 mm in length.

The CSB analog was comprised of no. 30 polycarbonate foam (Young's modulus 445 MPa) and short fiber filled epoxy shell (Young's modulus 157 GPa, density 0.48 g/cm^3; Sawbones, Vashon, Washington). This foam analog is used in human orthopedic studies to represent normal bone quality.[13] The foam density was 0.48 g/cm^3 and the cortical shell thickness was estimated from a computed tomography (CT) of a yearling Thoroughbred.[6] A 3D printed polylactic (PLA) acid analog (Young's modulus 2004 ± 63 MPa)[14] was designed using Tinkercad by Autodesk (© 2020 Autodesk, Inc.) and exported to Ultimaker Cura (Ultimaker B.V., Utrecht, the Netherlands; Version 4.5) for printing. Infill density was set at 55% with a tri-hexagonal infill pattern to model the cancellous bone and a 2 mm solid shell modeled cortical bone (Figure 3). Similar PLA 3D printed models of corticocancellous architecture perform comparably in mechanical testing as human vertebra.[15] These materials, used in other bone studies, were then custom designed to mimic bone engaged by a transcondylar screw across an MFC void based on measurements from computed tomographic imaging of a yearling Thoroughbred. The selection of 10 mm of bone thickness on either side of the void corresponded with the lower end of bone thickness measured at screw placement surgery in yearlings (E.M. Santschi, unpublished data).

2.2 | Digital measuring devices

The compression donut sensor was a flat 38 × 12.6 mm cylinder with a 4.6 mm central hole for the 4.5 mm fully threaded cortical screw to pass through. The sensor was connected to a digital gauge (ZTS-LMS-1100-062916-2;

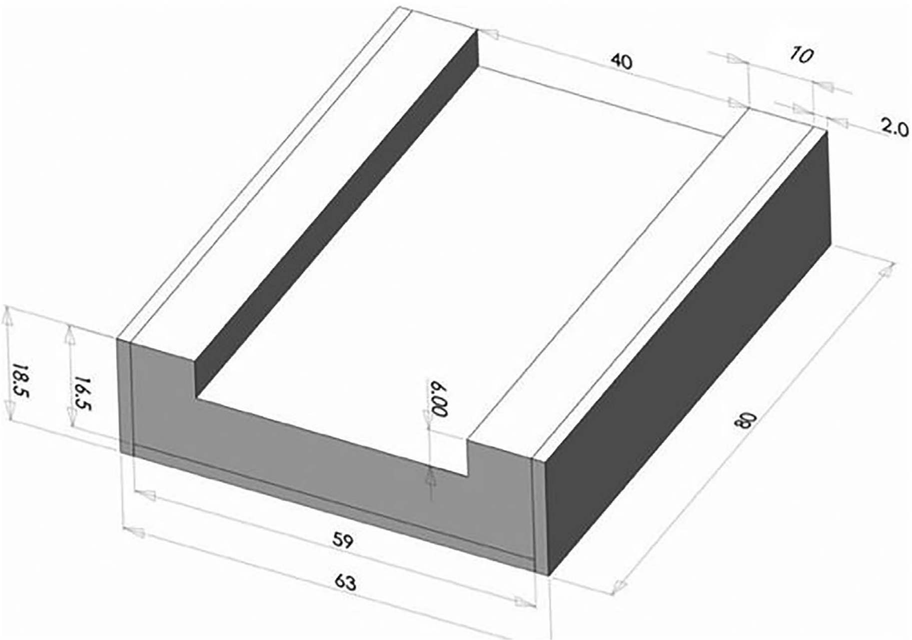

FIGURE 1 Draft rendering of composite bone analog. The exterior shell is the 2 mm thick cortical bone mimic, and the inner material is the 10 mm thick cancellous bone mimic. Polylactide analogs were the same dimensions. Measurements are in mm (image courtesy of Sawbones, Vashon, Washington)

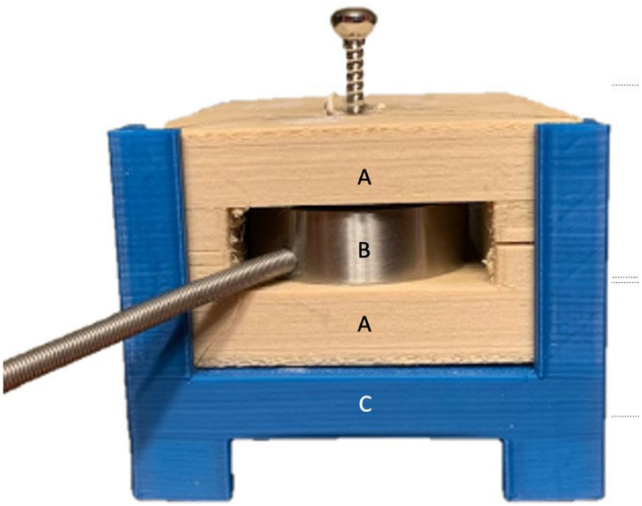

FIGURE 2 Test specimen assembly of 3D printed polylactic acid blocks. The dense exterior shell is the cortical bone mimic and the interior cancellous bone. A are blocks; B is the compression sensor and C is a 3D printed bracket used to maintain block alignment. 3D, three-dimensional

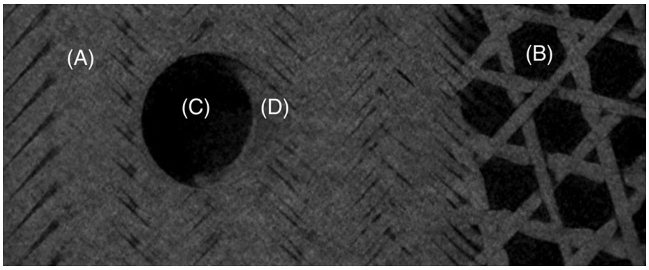

FIGURE 3 Microcomputed tomography image perpendicular to screw axis of 3D printed block after removal of a bicortical lag screw. A = cortical analog, B = cancellous analog, C = drilled path for screw tip, D = intact material tapped to engage screw threads. 3D, three-dimensional

Imada, Inc., Northbrook, Illinois) that recorded compression (N) and was collected on a laptop computer using purpose-made software (WinWedge by TALtech). Insertional screw torque was measured with a digital torque screwdriver (DIS-RL 10; Imada, Inc.).

2.3 | Screw insertion

A 3D printed bracket (Figure 2) maintained alignment of the two analogs. Fully threaded 4.5 mm cortical screws were used for all trials. As the screws were not countersunk, the head did not engage the model except at its underside. As a result, the 38 mm unicortical screw had 33 mm engaging the model and the 42 mm bicortical screw had 37 mm of engagement. The four screw conditions tested were lag with bicortical or unicortical engagement (LB and LU) and neutral with bicortical or unicortical engagement (NB and NU). The trials were run individually and the screw condition (1–4) was determined by random number generator until six trials of each type (NB, LB, NU, LU) were accomplished. This was performed in each analog, 24 trials per analog (PLA and CSB). Unicortical was defined as 80% of the transcancellous bone segment being engaged by the screw. PLA shims were placed under the sensor as needed to achieve uniform contact of the CSB blocks, as not all were cut the same resulting in a 0.5–1 mm gap based on the manufacturer's reported margin of error, which appeared to be mostly the cancellous bone component. The PLA analogs were printed with higher accuracy and did not require shims. All screws were placed by the same surgeon (CRM). The screws were tightened with a standard screwdriver until contact was made with the sensor, then further tightened to 2 Nm torque using a torque measuring screwdriver. This torque value was selected because stripping torque in no. 30 PCF foam is 2.7 Nm,[16] and ideal screw insertion torque is considered 70%–80% of max torque.[17,18]

2.4 | Cadaver bone trials

To estimate the compression in juvenile equine cancellous bone, one screw for each condition was placed ex vivo in the distal epiphyseal femoral bone of two 8-month-old Thoroughbred horses. The bones had been frozen at −80°C after use in a previous study using the medial femoral condyles; therefore, the lateral femoral condyles (LFC) were used. The LFC were drilled with a 3.2 mm drill bit in a lateral to medial direction, 15 mm proximal to the joint, in a similar fashion to the clinical scenario. The condyle was cut with a hand saw parasagittally so that the axial LFC bone was 10 mm thick. Cortical lag screws were placed in standard lateral to medial fashion with the compression sensor between bone sections. Screw length was determined by screw condition: bicortical screws engaged the medial cortical bone of the condyle and unicortical screws engaged 80% of the transcancellous bone segment. Previously fashioned 3D printed PLA shims were placed on either side of the sensor between the bone pieces to provide feedback resistance to compression and screws were tightened to 2 Nm torque.

2.5 | Data acquisition

For all trials, compression was measured at 3 s intervals for 12 h and recorded on a laptop computer. Specific measurements at 0, 0.5, 1, 2, 6, and 12 h were recorded in a separate table for analysis. Micro CT examinations were performed on PLA blocks after screw removal to examine the structural changes created during screw insertion. The micro-CT was performed by a Skyscan 1172-D (Kontich, Belgium) with a 27 × 27 × 27 μm^3 voxel size at 50 kVp, 200 μA, at 0.4° rotation per projection, six frames averaged/projection, 500 ms exposure time. The raw scan images were reconstructed into a three-dimensional data set by using a reconstruction software (NRecon v1.6.1.0; Bruker, Kontich, Belgium) followed by analysis in ImageJ (ImageJv1.8.0; NIH, Bethesda, Maryland).

TABLE 1 Median compression and interquartile range (IQR, $n = 6$) in Newtons (N) for each screw condition in polylactic acid (PLA) printed blocks and composite synthetic bone (CSB) blocks over time after placement

	0 h (N) Median (IQR)		0.5 h (N) Median (IQR)		1 h (N) Median (IQR)		2 h (N) Median (IQR)		6 h (N) Median (IQR)		12 h (N) Median (IQR)	
Screw	PLA	CSB	PLA	CSB	PLA	CSB	PLA	CSB	PLA	CSB	PLA	CSB
NB	607 (328)	326 (110)	471 (309)	246 (95)	451 (304)	233 (94)	428 (297)	226 (103)	391 (275)	209 (99)	372 (254)	212 (84)
LB	876 (177)	427 (302)	427 (271)	306 (117)	390 (257)	284 (101)	351 (238)	272 (111)	302 (140)	257 (107)	313 (207)	264 (101)
NU	396 (162)	347 (65)	237 (90)	231 (56)	225 (83)	225 (55)	211 (76)	217 (55)	185 (60)	202 (53)	164 (54)	196 (55)
LU	573 (210)	338 (218)	321 (146)	271 (133)	294 (139)	258 (124)	268 (126)	243 (123)	222 (90)	232 (110)	186 (61)	226 (88)

Note: There were 24 total trials in each analog, six replicates per screw-analog combination. NB, neutral bicortical; LB, lag bicortical; LU, lag unicortical, NU: neutral unicortical. The IQR represents the difference between the 75th and 25th percentiles of the data at each time point. This data is graphically represented in Figure 4.

TABLE 2 Median values and interquartile range (IQR) in Newtons (N) per group (including all time points) with associated Kruskal–Wallis *p*-value

	PLA				CSB			
Screw type	**NB**	**LB**	**NU**	**LU**	**NB**	**LB**	**NU**	**LU**
Median (N)	437	379	208	265	247	293	228	261
IQR (N)	317	294	105	154	111	159	77	123
p-value	0.0001				0.02			

Note: There were 24 total trials in each analog, six replicates per screw-analog combination. NB, neutral bicortical; LB, lag bicortical; LU, lag unicortical; NU, neutral unicortical. The IQR was calculated using STATA using all 36 values (6 values × 6 time points) for each screw type. This data is graphically represented in Figure 5.
Abbreviations: CSB, composite synthetic bone; PLA, polylactic acid.

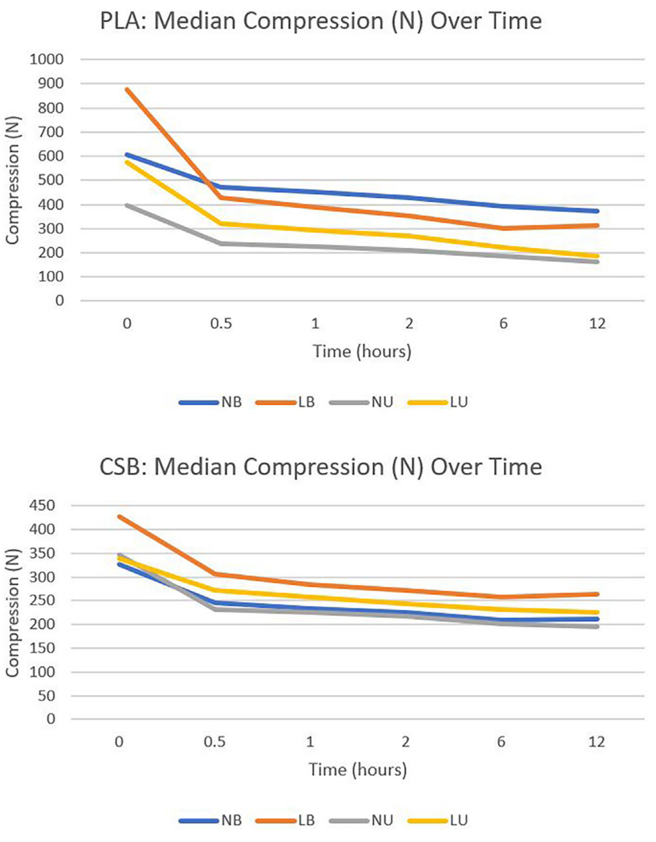

FIGURE 4 Change in compression (N) over 12 h by screw type

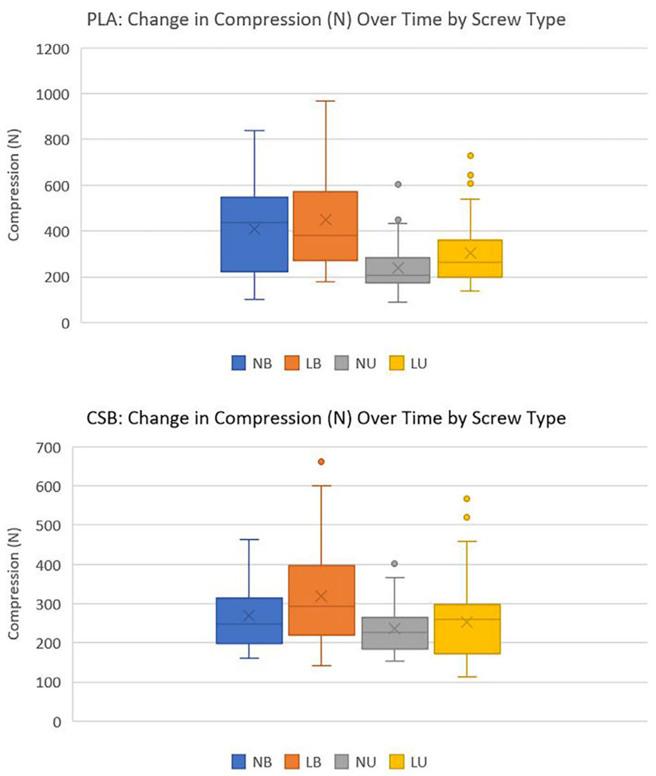

FIGURE 5 Box plot of total data set—compression (N) by screw type

2.6 | Statistical analysis

Sample size (six trials per screw condition) was estimated based on previously published data using bone analogs and the minimum size needed ($n = 5$) for calculation of accurate *p*-values when comparing three or more independent groups.[19,20] Data were analyzed using Stata/MP 13.0 for Windows (StataCorp LP, College Station, Texas). A Doornik-Hansen test for multivariate normality was performed and the data were not normal. The Kruskal-Wallis test was conducted for each analog (PLA and CSB) on the four screw conditions to examine the effect of screw condition on compression. When a difference was significant, Dunn-Bonferroni adjusted *p*-values were used to compare differences between the four groups (lag bicortical screw [LB], lag unicortical screw [LU], neutral bicortical screw [NB], and neutral unicortical screw [NU]). Significance for both tests was set at $p < .05$. Data were also evaluated for loss of compression on a percentage basis over time, but these values are strictly descriptive.

Stata/MP 13.0 was utilized to calculate the interquartile range for each screw condition as listed in

TABLE 3 Comparisons between screw conditions (Dunn-Bonferroni)

PLA comparisons						
	NB:LB	NB:LU	NB: NU	LB:LU	LB:NU	LU:NU
p-value	1.000	*0.0752*	*<0.001*	*0.012*	*<0.001*	0.181
CSB comparisons						
	NB:LB	NB:LU	NB: NU	LB:LU	LB:NU	LU:NU
p-value	0.426	1.0	0.375	0.768	*0.008*	1.000

Note: Statistically significant *p*-values are italicized.
Abbreviations: CSB, composite synthetic bone; PLA, polylactic acid.

TABLE 4 Percent change in compression between time points by screw condition and material type

	Start to 1 h		1–6 h		6–12 h		Start to 12 h	
Screw condition	PLA	CSB	PLA	CSB	PLA	CSB	PLA	CSB
Neutral bicortical	−26%	−29%	−13%	−10%	−5%	+1%	−39%	−35%
Lag bicortical	−55%	−33%	−23%	−10%	+4%	+3%	−64%	−38%
Neutral unicortical	−43%	−35%	−18%	−10%	−11%	−3%	−58%	−43%
Lag unicortical	−49%	−24%	−24%	−10%	−16%	−3%	−67%	−33%

Abbreviations: CSB, composite synthetic bone; LB, lag bicortical; LU, lag unicortical; NB, neutral bicortical; NU, neutral unicortical; PLA, polylactic acid.

TABLE 5 Compression (Newtons) measured in cadaver femoral bone

Screw condition	0 h (N)	0.5 h (N)	1 h (N)	2 h (N)	6 h (N)	12 h (N)	Compression change (start-12 h)
Neutral bicortical	272	207	204	200	193	187	−31%
Lag bicortical	316	141	138	136	129	125	−60%
Neutral unicortical	276	178	176	173	167	163	−41%
Lag unicortical	381	109	106	103	98	95	−75%

Note: One trial was performed per screw condition (6 total).

Tables 1 and 2. Not all statistical software use the same method for quantile estimation and different values might be obtained using other programs. Furthermore, Excel should not be used for quantile estimation of small data sets.

3 | RESULTS

Stripping of screws was not detected manually in any trial. Compression was greatest at screw insertion (0 h) and decreased over time in all screw conditions (Tables 1 and 2, Figures 4 and 5). Changing the screw condition resulted in detectable differences in compression (N) for the PLA analog ($p < .001$) and the CSB analog ($p = .02$) (Tables 1 and 2). For the PLA analog, a difference was detected between the NB screw (median 437 N, interquartile range [IQR] 317 N) and the NU screw (median 208 N, IQR 105 N, $p < .001$), the LB screw (median 379 N, IQR 294 N) and the NU screw ($p < .001$), and the LB screw and LU screw (median 265 N, IQR 154 N, $p = .01$) (Table 3). For the CSB analog, the LB screw (median 293 N, IQR 159 N) and the NU screw (median 228 N, IQR 77 N) differed ($p = .008$, Table 3). Medians did not differ significantly between the NB and LB screw in either model. Median compression (N) decreased for all screw conditions and in both analogs over 12 h, with the greatest loss of compression occurring in the first hour (Table 4).

Compression was measured in four cadaver distal femoral epiphyseal femurs in one trial of each screw condition to determine the similarity of analogs to bone. Compression (N) generated in cadaver condyles at all time periods (Table 5) was lower than in the bone models. Compression retained by a cadaver stifle over 12 h ranged from 69% for one NB screw to 25% with a LU screw. The largest compression losses over the 12 h were noted in the LU screw (60%) and the LB screw (75%).

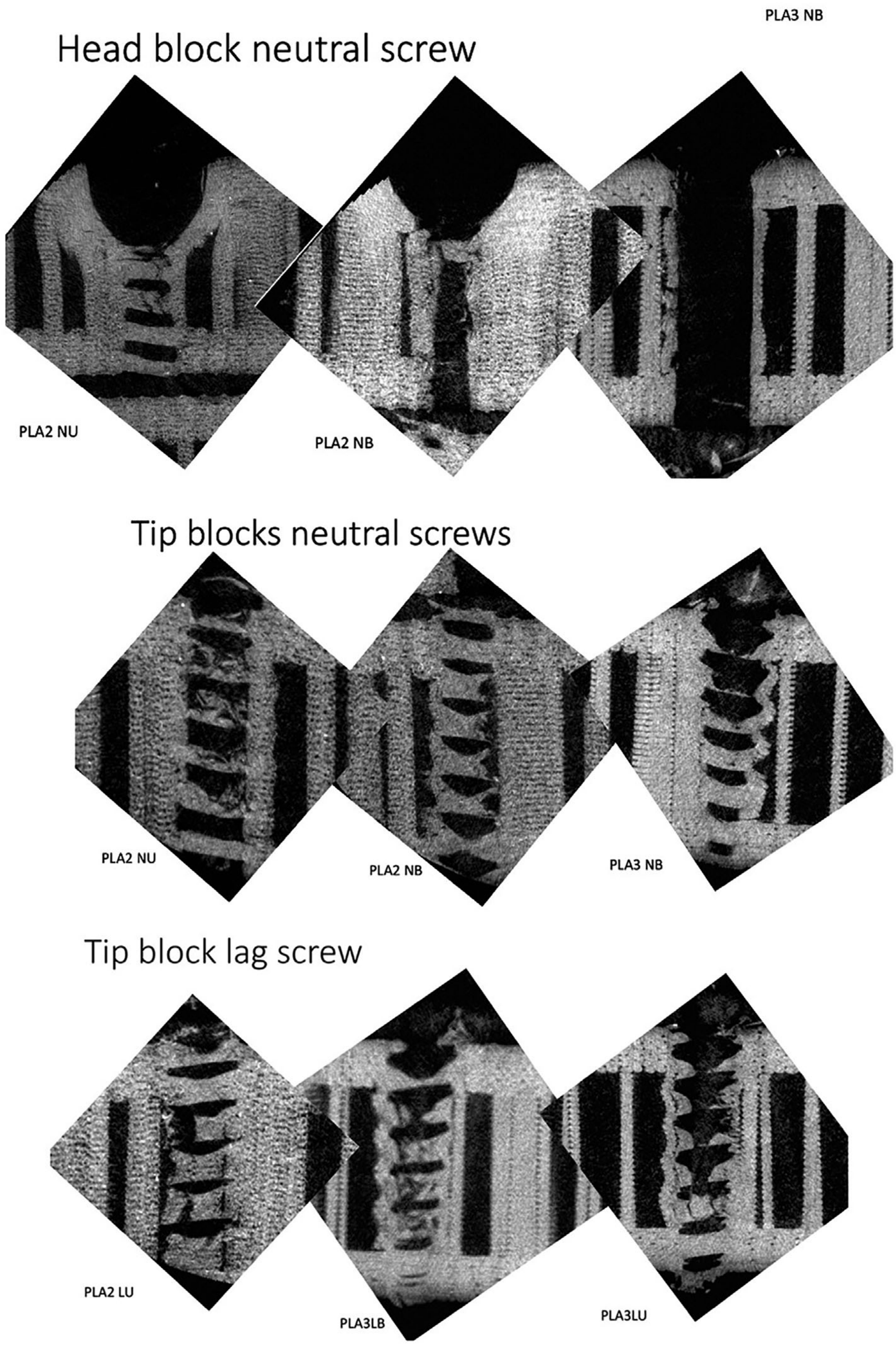

FIGURE 6 Long axis slice images of parasagittal screw paths in polylactic acid 3D printed analogs. The images were 1–2 mm off the central axis of the screw. 3D, three-dimensional

This is consistent with the PLA model in which 67% of the compression (N) was lost over 12 h with the LU screw and 64% with the LB screw (Table 4).

Six PLA test specimens (three lag and three neutral screws) were evaluated with micro-CT as the CSB blocks could not be imaged by the available equipment. Neutral screws caused crushing at the head contact surface or between screw threads in the head block. In the tip block, there was minor disruption of the threads (Figure 6). Lag screws had a smooth glide path in the head block with minimal surface crushing. There was mild to moderate disruption of tip block threads and vertical cracking between and around the threads (Figure 6).

4 | DISCUSSION

As we hypothesized, neutral screws generated compression (N) across the analogs with either unicortical or bicortical engagement. In CSB, compression was not statistically different between LB, LU, and NB screws.

However, there was a statistical difference between LB and NU screws. In PLA, compression was not statistically different for NB and LB screws, but was different for NB and NU screws, LB and NU screws, and LB and LU screws. These results are in agreement with a previous study in which fully threaded 7.0 mm screws achieved the same interfragmentary compression through cancellous bone as partially threaded screws.[12] Although our clinical impression prompted our hypothesis, the absence of difference between neutral and lag screws was surprising, as contrary to general knowledge.[9] This difference is likely because most screw mechanics has been studied in cortical bone, which is different from cancellous bone.

The results of this study suggest that bicortical screw engagement produces statistically higher levels of compression compared to unicortical screw engagement. Previous studies have indicated that bicortical engagement increases screw compression experimentally[21] and reduced screw loosening in vivo.[22] Because the difference in this study occurred mostly at the 6- and 12-h measurements, the primary effect of bicortical engagement may be to maintain compression over time. This result was most consistent in the PLA analog (differences detected in NB:NU, LB:NU, LB: LU) and less so in the CSB analog (difference detected in LB:NU only). The exact source of these differences between the analogs is unknown but may be related to different material properties. As screw compression increases with bone density,[23] there is greater compression generated by screws in PLA blocks as compared to CSB as the result of an increase in material density because the maximum torque and the screws were the same. The lesser compression in the cadaver bones is probably due to reduced bone density in 8-month-old horses. The authors realize that multiple comparisons can increase the likelihood of type 1 error. This was minimized by the use of the Bonferroni adjustment.

Published studies measuring screw compression in cancellous bone analogs or cadaveric bone are uncommon and do not evaluate compression over time. In this study, screws had the highest peak compression at time 0 with a rapid decline over 30 min followed by a much slower decrease to 12 h. When trabecular bone is compressed to failure (yield point), the structure unloads to a residual strain.[24] This permanent deformation of a material is termed creep and is time-dependent, starting at a rapid rate and slowing over time,[25] similar to the loss of compression in this study. Creep is a common failure mode in trabecular bone[24,25] and probably is a major factor in the loss of compression.

Calculation of the median percentages of compression retained for the four screw conditions from 1 to 12 h revealed that CSB (57%–67%) had numerically greater compression retention than PLA (33%–61%), although these values were not statistically evaluated. Cadaver bone had a range of 25%–69% compression retention which appeared more similar to PLA, but cannot be critically evaluated as it was limited to a very small sample. The general trend was that the neutral bicortical screw retained the most compression, and the lag unicortical screw the least. Fully threaded screws can generate more compressive force due to greater thread purchase[26] and we speculate may reduce the loss of compression.

The limited micro-CT images available indicate how neutral screws achieve compression. Compression with a neutral screw was achieved by compressing the outer shell and stripping of the threads in the near block, similar to fully threaded cannulated screws.[12] The tip block threads were relatively intact. Compression with a lag screw appeared to be achieved by gliding through the head block and drawing the tip block to the head block; screw threads were relatively undisturbed, but vertical delamination of the tip material was apparent. Analog damage present suggested that the screws were overtightened and may have contributed to compression loss, despite being approximately 75% of stripping torque. Further studies with varying torque limits could help determine an ideal torque for screw insertion in cancellous bone and the method of failure.

In this study, achieving high initial compression did not result in increased compression at 12 h. We believe that compression is an important factor for sustained bone formation stimulus in an MFC SCL, and a long-term goal is to describe the ideal screw mechanics for this purpose. This study is a first step in determining those methods but has several limitations. To model the clinical scenario, the model should reflect the shape of the MFC with a void, the time interval should be extended, from 12 to 24 h and beyond to determine at what point the compression plateaus. Our primary goals in this foundational study were to model the density and thickness of the MFC bone engaged by the screw across a void and accurately measure compression generated by a screw like those used in equine surgery. Other parameters such as weight bearing and joint kinematics may have an impact and were not evaluated in this study. It may also be valuable to evaluate compression over a longer measurement period. This study utilized two bone models that have been used in previous mechanical experiments. The use of bone analogs provides consistency within the experiment, limiting natural variation present in real bone. Additionally, cadaver bone from appropriately aged animals is limited and only one trial can be performed per femoral condyle. There is also the challenge of creating a consistent void within the bone and accommodating the sensor. These challenges were overcome by designing bone analogs to mimic the MFC, but this may not precisely mimic the MFC in vivo. Other bone models should be considered as more information is gathered about this unique anatomical area. Furthermore, validation of these findings in equine cancellous bone may help create clinical guidelines and improve surgical outcomes.

In conclusion, neutral screws can be used to generate compression in cancellous bone analogs and in cadaver bone. Compression was better maintained over 12 h if two cortices of bone analog were engaged. Compression generated by screws in cancellous analogs and juvenile cadaver bone declines up to 12 h after screw insertion. A better understanding of how screws impact compression in the MFC requires further investigation before making clinical recommendations.

ACKNOWLEDGMENTS

Author Contributions: Caitlin R. Moreno: Project design and primary experimenter. Significantly contributed to drafting of the manuscript. Elizabeth M. Santschi: Contributed expertise in this area of study. Helped with study design and manuscript drafting. Jennifer Janes: Contributed mechanical testing knowledge and helped with manuscript preparation. Jie Liu: Performed the micro-CT imaging of the PLA analogs and contributed to manuscript preparation. Do-Gyoon Kim: Contributed expertise in micro-CT and helped with manuscript preparation. Alan S. Litsky: Contributed mechanical testing knowledge as applicable to this anatomic area of interest and helped with drafting of the manuscript.

CONFLICT OF INTEREST

The authors have no conflicts of interest to declare.

FUNDING INFORMATION

Kansas State University, Department of Clinical Sciences

The results of this study were presented at the ACVS Surgery Summit 2020.

ORCID

Caitlin R. Moreno https://orcid.org/0000-0001-5456-4520

REFERENCES

1. Baxter GM. Subchondral cystic lesions in horses. In: McIlwraith CW, Trotter GW, eds. *Joint Disease in the Horse*. Saunders; 1996:384-397.
2. Santschi EM. Treatment options and long-term outcomes of horses with subchondral lucencies of the medial femoral condyle. *Equine Vet Educ.* 2021;33:386-388.
3. Santschi EM, Williams JM, Morgan JW, Johnson CR, Bertone AL, Juzwiak JS. Preliminary investigation into the treatment of equine medial femoral condylar subchondral cystic lesions with a transcondylar lag screw. *Vet Surg.* 2015;44: 281-288.
4. Roquet I, Easter JL, Coomer RPC, et al. Treatment of subchondral lucencies in the medial proximal radius with a bone screw in eight horses. *Vet Surg.* 2017;46:478-485.
5. Santschi EM, Whitman JL, Prichard MA, et al. Subchondral lucencies in the proximal tibia of 17 horses. *Vet Surg.* 2020;49: 778-786.
6. Frazer LL, Santschi EM, Fischer KJ. Impact of a void in the equine medial femoral condyle on bone stresses and peak contact pressures in a finite element model. *Vet Surg.* 2019;48: 237-246.
7. Frazer LL, Santschi EM, Fischer KJ. Stimulation of subchondral cyst healing by placement of a transcondylar screw in the equine medial femoral condyle. *Vet Surg.* 2019;48:1194-1203.
8. Perren SM, Cordey J, Baumgart F, Rahn BA, Schatzker J. Technical and biomechanical aspects of screws used for bone surgery. *Int J Ortho Trauma.* 1992;2:31-48.
9. Uhl RL. The biomechanics of screws. *Ortho Rev.* 1989;18:1302-1307.
10. Fletcher JWA, Ehrhardt B, MacLeod A, Whitehouse MR, Gill H, Preatoni E. Non-locking screw insertion: no benefit seen if tightness exceeds 80% of the maximum torque. *Clin Biomech.* 2019;70:40-45.
11. Nunamaker DM. General techniques and biomechanics. In: Fackelman GE, Auer JA, Nunamaker DW, eds. *AO Principles of Equine Osteosynthesis*. AO Publishing; 2000:11-25.
12. Eastman J, Deafenbaugh B, Christiansen B, Garcia-Nolen T, Lee M. Achieving interfragmentary compression without special drilling technique or screw design. *J Orthop Res.* 2018;36: 1099-1105.
13. Diaz MA, Garrigues GE, Ricchetti ET, Gutierrez S, Frankle MA. Relationship between insertion torque and compression strength in the reverse total shoulder arthroscopy baseplate. *J Ortho Res.* 2020;38:871-879.
14. Kamthai S, Magaraphan R. Thermal and mechanical properties of polylactic acid (PLA) and bagasse carboxymethyl cellulose (CMCB) composite by adding isosorbide diesters. *AIP Conference Proceedings*. 2015;1664:060006.
15. Bohl MA, Morgan CD, Mooney MA, et al. Biomechanical testing of a 3D-printed L5 vertebral body model. *Cureus.* 2019;11: e3893.
16. Acker WB, Tai BL, Belmont B, Shih AJ, Irwin TA, Holmes JR. Two-finger tightness: what is it? Measuring torque and reproducibility in a simulated model. *J Orthop trauma.* 2016;30: 273-277.
17. Cleek TM, Reynolds KJ, Hearn TC. Effect of screw torque level on cortical bone pullout strength. *J Orthop Trauma.* 2007;21: 117-123.
18. Fletcher JWA, Zderic I, Gueorguiev B, et al. Stripping torques in human bone can be reliably predicted prior to insertion with optimum tightness being found between 70% and 80% of the maximum. *Bone Joint Res.* 2020;9:493-500.
19. Moreno CR, Santschi EM, Younkin JT, Larson RL, Litsky AS. The failure mode of a mechanically loaded equine medial femoral condyle analog with a void and the impact of lag and neutral screw placement. *Vet Surg.* 2022. doi:10.1111/vsu.13765

20. Chan Y, Walmsley RP. Learning and understanding the kruskal-wallis one-way analysis-of-variance-by-ranks test for differences among three or more independent groups. *Phys Ther*. 1997;77(12):1755-1761.
21. Park J-W, Kim K-T, Sung J-K, Park S-H, Seong K-W, Cho D-C. Biomechanical comparison of inter-fragmentary compression pressures: lag screw versus Herbert screw for anterior odontoid screw fixation. *J Korean Neurosurg*. 2017;60:498-503.
22. Ricci WM, Tornetts P, Borrelli J. Lag screw fixation of medial malleolar fractures; a biomechanical, radiographic, and clinical comparison of unicortical partially threaded lag screws and bicortical fully threaded lag screws. *J Orthop Trauma*. 2012;26:602-606.
23. Okazaki Y, Hayakawa E, Tanahashi K, Mori J. Mechanical performance of metallic bone screws evaluated using bone models. *Materials*. 2020;13:4836.
24. Oftadeh R, Perez-Viloria M, Villa-Camacho JC, Vaziri A, Nazarian A. Biomechanics and mechanobiology of trabecular bone: a review. *J Biomech Eng*. 2015;137(010802):1-15.
25. Bowman SM, Keaveny TM, Gibson LJ, Hayes WC, McMahon TA. Compressive creep behavior of bovine trabecular bone. *J Biomech*. 1992;27:301-310.
26. Patel P, Tiedeken N, Qvick L, Debski RE, Kaufman R, Fowler JR. Interfragmentary compression forces vary based on scaphoid bone screw type and fracture location. *Hand*. 2019;14:371-376.

How to cite this article: Moreno CR, Santschi EM, Janes J, Liu J, Kim D-G, Litsky AS. Compression generated by cortical screws in an artificial bone model of an equine medial femoral condylar cyst. *Veterinary Surgery*. 2022;51(5):833-842. doi:10.1111/vsu.13814